

Variations of the glacier mass balance and lake water storage in the Tarim Basin, northwest China, over the period of 2003–2009 estimated by the ICESat-GLAS data

Ninglian Wang^{1,2} · Hongbo Wu^{3,4} · Yuwei Wu^{3,4} · Anan Chen^{3,4}

Received: 11 February 2015 / Accepted: 13 June 2015 / Published online: 26 June 2015
© Springer-Verlag Berlin Heidelberg 2015

Abstract Accurately estimating the changes in glacier mass balance and water storage in lakes and reservoirs is critical to studying the water cycle in the inland river basin in northwest China. We used high-resolution satellite images to analyze the changes in water surface area of lakes and reservoirs in Tarim Basin, and used the ICESat-GLAS altimeter data to estimate their water level changes and the glacier mass balance change, over the period 2003–2009. The results showed the average glacier thinning in the entire basin was at a rate of 0.34 ± 0.25 m w.e./year equivalent height of water, which means that the glacier mass balance occurred -6.8 ± 1.2 km³ water equivalent over the study period. However, the mean water level of nearby lakes decreased by 0.41 ± 0.2 m even with the influx of glacial melt water, indicating that the lake level declines were caused by the withdrawal of lake water for human activities.

Keywords ICESat-GLAS · Glacier mass balance · Elevation change · Tarim Basin · Lakes water storage

Introduction

Variations in the water volume storage of inland lakes and reservoirs reflect both the input of climate change and human activity on terrestrial water resources (Calmant and Seyler 2006), which is fundamental for understanding the lakes water balance, sea level rise variations (Wisser et al. 2013), and glacial runoff response to extreme climatic events, such as abrupt changes in air temperature, floods, snowfall, and drought (Sorg et al. 2012). Both inland lakes and exorheic lakes, are very sensitive to climate change (Crétaux et al. 2011). The inland arid regions are especially sensitive to variations in water resources with the threat of global warming (Zhang et al. 2010). Therefore, observations of water storage (mostly area and water level) in lakes and rivers have been carried out in most developed countries since 1993 (Alsdorf et al. 2007). Furthermore, the inland lakes are more sensitive to variability of surface water resource utilization and shortage. The mountain glaciers in the upstream of the Tarim River, northwest China, are important for the water supply of the downstream oases. These oases have already been potentially affected by climate change (Beniston 2003), but to what extent is unclear yet (Immerzeel et al. 2010).

So far, the satellite laser ranging (SLR) techniques, with centimeter accuracy, have become a powerful tool in monitoring inland water resources (Lemoine et al. 2010), especially for the non-monitored waterbodies (rivers, lakes, reservoirs, floodplains, and wetlands) at regional and global scales (Calmant et al. 2008). Current understanding on the global abundance and size distribution of lakes comes from two sources; map compilations and statistical extrapolations based on abundance-size relationships (Verpoorter et al. 2014). Water mass balance is an essential aspect of

✉ Hongbo Wu
hongbowu2010@hotmail.com

¹ Cold and Arid Regions Environmental and Engineering Research Institute, Chinese Academy of Sciences, Lanzhou 730000, People's Republic of China

² CAS Center for Excellence in Tibetan Plateau Earth Sciences, Beijing 100101, People's Republic of China

³ State Key Laboratory of Cryospheric Sciences, Cold and Arid Regions Environmental and Engineering Research Institute, Chinese Academy of Sciences, Lanzhou 730000, People's Republic of China

⁴ University of Chinese Academy of Sciences, Beijing 100049, People's Republic of China

water management activities (Biemans et al. 2011). Lake water level and storage variations indicate the state of the water mass balance in an inland basin. Space-borne altimeters (Jason-1, Envisat Radar Altimeter, RadarSat-1, GEOSat, GFO, Jason-2, T/P, ICESat-GLAS, CryoSat, etc.) have been successfully used to measure lakes, reservoirs, rivers, and wetland variations in the past decade (Medina et al. 2008; Santos da Silva et al. 2010). Due to the time bias differences demonstrated by a robust linear fit with the mean along-track differences in the orbits (Zelensky et al. 2006), the temporal and spatial variations in lake water discharge and storage changes are estimated from time-varying gravity (Landerer and Swenson 2012; Moiwu et al. 2011) and SLR satellite altimeter data (Llovel et al. 2010; Zelensky et al. 2014).

The Geoscience Laser Altimeter System (GLAS) onboard the Ice, Cloud, and land Elevation Satellite (ICESat) can be applied to derive the surface elevation data of lakes (Phan et al. 2012) and reservoirs (Song et al. 2014). The ICESat elevation measurement accuracy is only about 5 cm (Baghdadi et al. 2011), which means that some lakes and reservoirs could be monitored using ICESat footprints tracks with acceptable accuracy. Although the continuous GLAS footprint values have high frequency autocorrelations (Abdallah et al. 2011), mean lake water levels increased by 0.23 m/year for the 56 salt lakes and 0.27 m/year for the 50 salt lakes in the Tibetan Plateau in recent years (Zhang et al. 2011). The GLAS-estimation of reservoir storage and its variations in South Asia also correlates with in situ data and radar altimetry (Zhang et al. 2014). In the past 40 years, glacier meltwater has significantly influenced water resources in the Tarim basin (Liu

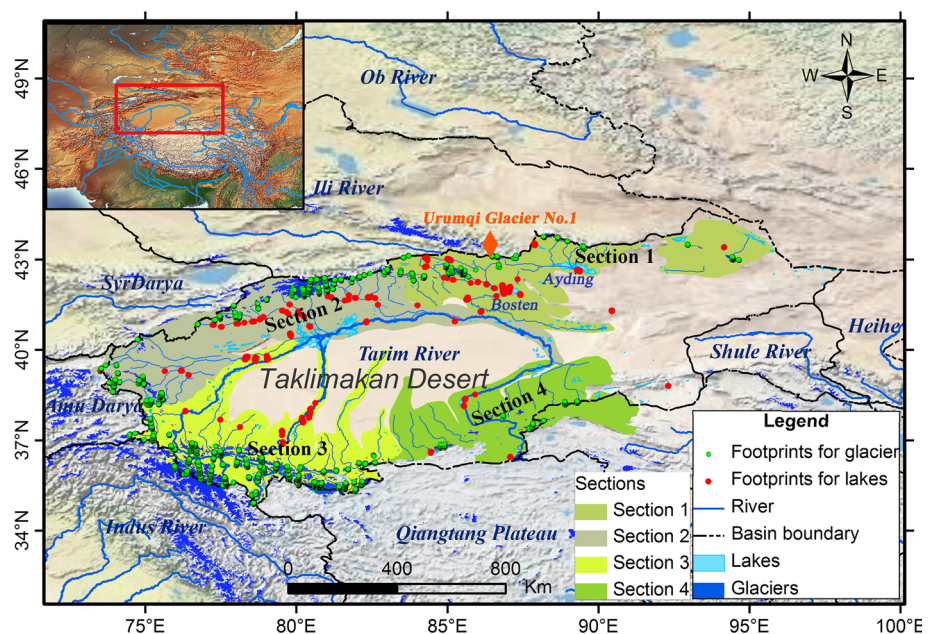
et al. 2006). The runoff of the Tarim River and its tributaries showed an increased trend over the past decades, which cannot be explained by precipitation alone, and suggests a significant contribution from glacier meltwater (Piao et al. 2010). In order to understand the relationship of lake water mass balance and glacier meltwater variations in the Tarim Basin, this paper presents the variations in water levels, lake volume storage and glacier mass balance in the entire Tarim Basin derived from GLAS data over the period 2003–2009.

Data and methods

Study area

The Tarim Basin is the largest inland basin in China, with an area of 1.19×10^6 km², of which the mountainous area (≥ 2500 m a.s.l.) is about 350,000 km². It spans about 2000 km from east to west and 800 km from north to south, and is surrounded by the Tianshan Mountains, Kunlun Mountains, and Altun Mountains (see Fig. 1). The extremely arid climate makes the Tarim Basin to be the largest desert in China (Zhao et al. 2013b) where the major part of the basin is covered by the Taklamakan Desert. Based on the latest Randolph Glacier Inventory (RGI 3.2) from Global Land Ice Measurements from Space (GLIMS) project (Raup et al. 2007a, b), these 14 285 glaciers with an area of 21×10^3 km² exist in the surrounding mountains of the Tarim Basin, which provide the major water source with human activities and natural ecosystems in the lower catchment of the basin (Qi et al. 2005). The Tarim River is

Fig. 1 The location of Tarim River basin and the distributions of glaciers and lakes. The red circles represent the ICESat footprints located on the water surface and the green circles located on the glacier surface



the largest river in Tarim Basin, and composed by the Aksu River, Yarkand River, Hotan River, and Qarqan River. In addition, the downstream areas of Tarim River is an important agricultural production region (Li and Williams 2008).

GLAS data

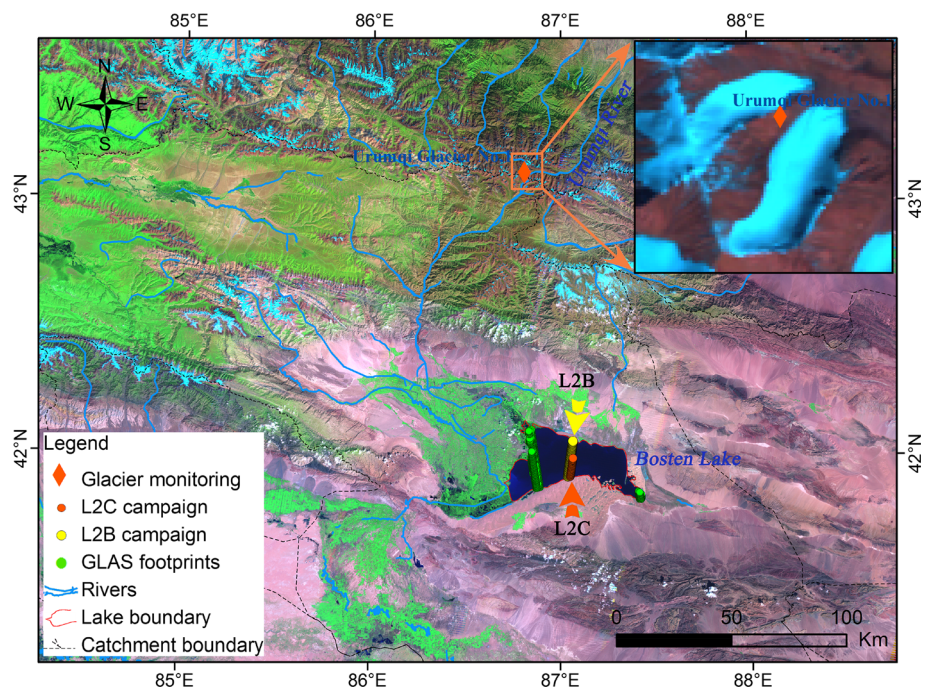
ICESat-GLAS measurements will employ 1064-nm laser pulses to measure the heights of the land surface, forest area and dense cloud and 532 nm pulses for measuring the vertical clouds and aerosols distribution (Zwally et al. 2002). Each GLAS footprint, with a diameter of ~70 m and with an along-track spacing of 170 m, has a surface-ranging accuracy of 10 cm (Schutz et al. 2005). The 532-nm pulse profiles have much better sensitivity than the 1064-nm profiles for aerosol backscatter and are available for all operation periods (Abshire et al. 2005). GLAS data were requested and downloaded from the National Snow and Ice Data Center (NSIDC, <http://www.nsidc.org/data/icesat/order.html>), and the latest altimetry products are Release 34. The GLA01 product is one of 15 GLAS products, where the returned waveform contains 544 bins with various peaks fitted by Gaussian curves. GLA14 parameters, i.e., elevation, latitude, and longitude values (Los et al. 2012), are corrected saturation elevation due to slope and roughness (Li et al. 2012). The ICESat satellite laser data were processed in Matlab for precise orbit determination (POD) and for estimating station positions.

Lake water level and glacier mass balance

The water levels and volumes of many lakes are routinely monitored weekly in situ measurements and space-borne satellite altimeters. Their time series data can be obtained from Laboratoire d’Etudes en Géophysique et Océanographie Spatiales (LEGOS, see <http://www.legos.obs-mip.fr/>), where the ERS-1/EnviSat and Jason-2 assess the lakes’ changes (Da Silva et al. 2011). The ESR-2/EnviSat, Jason-2 satellite water level time series dataset of Bosten Lake (42.01°N; 87.12°E) and Ayding Lake (42.66°N, 89.27°E) in observed data range and that the online topographic correction database system from the European Space Agency (ESA, <http://www.tethys.eaprs.cse.dmu.ac.uk/RiverLake/shared/main>) are all present between August 2002 and 2009. Our focus is to estimate the changes in water volume of lakes, which can be jointly done by the relative water level and area variations (Frappart et al. 2006b) and does not need their absolute values which are influenced by referencing (Crétaux and Birkett 2006).

The Urumqi Glacier No.1 at the source area of the the Urumqi River in the East Tianshan Mountains is located at 43.08°N, 86.82°E (close to Bosten Lake), see Fig. 2. The in situ measurements of glacier mass balance data, which can be downloaded from World Glacier Monitoring Service (WGMS, see the website <http://www.wgms.ch/gmbb.html>), is used to evaluate the reliability of the glacier mass balance estimated by the GLAS data. (Ye et al. 2005) demonstrate that both summer precipitation and air temperature negatively correlate with glacier mass balance and

Fig. 2 The locations of the Urumqi Glacier No. 1 at the source area of the Urumqi River and GLAS footprints on the Bosten Lake, Tarim Basin. The color image is combined with Band 5, Band 4, and Band 2 of TM/ETM data on the path/row (143/30, 142/31, 142/30, 144/31, 144/30, 141/31, 143/31)



are positively associated with glacial meltwater runoff. This correlation also indicates the summer temperature dominates on glacier mass balance and glacial runoff changes in Urumqi River (Jing et al. 2006).

Calculations of the changes in lake water level and water storage

A time series of Landsat TM/ETM images was employed to compare and describe the trend of lakes area changes (Kropáček et al. 2012). The available images scenes include no cloud covered scenes acquired by following Landsat sensors: Thematic Mapper (TM) and Enhanced Thematic Mapper Plus (ETM+), both with a resolution of 30 m. These mechanical optical scanners include green bands and near infrared bands (NIR), where the normalized difference water index (NDWI) is suitable for depicting lake and reservoir water bodies (McFeeters 1996). The Landsat image data were downloaded from Earth Resources Observation and Science (EROS) Center (USGS, <http://www.earthexplorer.usgs.gov/>). Accuracy of the co-registration was checked on a set of independent 150 points (RMSE = 20.1 m) for each scene, and was co-registered on the basis of Landsat scenes for July–August 2003.

Since the GLAS footprint elevation data were very limited, we could not directly combine the GLAS water elevation with the Landsat image water surface level area to calculate the water discharge in the small rivers. Therefore, the calculation of the changes in lake water level and water storage are as follows: (1) estimation of the water surface area based on NDWI images (the NDWI index ranges from -1 to 1 and the NDWI index value of defined water surface features from 0 to 1 .) during 2003–2009; (2) extraction of the mean lake surface elevations from GLA14 and GLA01 products data; (3) establishing the regression equation of the lake area and mean lake water level elevation for each lake/reservoir, and then fitting the water surface elevation value on the basis of the above established relationship; and (4) computing the increased/decreased lake water storage over the corresponding time span according to the time series of the GLAS-lake water surface elevation and lake area data (Frappart et al. 2006b). So, the change in lake water storage ΔV_{lakes} , can be estimated from the lake surface area and the area-elevation relationship using the following equation,

$$\Delta V_{\text{lakes}} = \frac{\bar{h}_{k+1} - \bar{h}_k}{3} (s_k + s_{k+1} + \sqrt{s_k \times s_{k+1}}), \quad (1)$$

where \bar{h}_k and \bar{h}_{k+1} are the mean lake water levels at two adjacent time spans, and s_k and s_{k+1} represent their corresponding surface areas. k is the j th campaign of GLAS footprints and the $k+1$ GLAS data from the next campaign.

The mean water level elevation is computed by the following equation,

$$\begin{aligned} \bar{h}_j &= \frac{1}{n} \left(\sum_{j=1}^n h_{j,\text{footprint}} + \sum_{j=1}^n e_{\text{overall}} \right) \\ &= \frac{1}{n} \sum_{j=1}^n h_{j,\text{footprint}} + \frac{1}{n} \sum_{j=1}^n e_{\text{overall}}, \end{aligned} \quad (2)$$

where $h_{j,\text{footprint}}$ is the elevation value of j th GLAS footprint for 18 GLAS data campaign. The variable n is the number of the GLAS footprints on the study lakes. The variable e_{overall} is the overall accuracy for each GLAS footprint including the GLAS track shift errors in each campaign, co-registration bias and uncertainty errors in EGM 2008 geoid model with WGS84 project coordinates (Hirt et al. 2010; Pavlis et al. 2012).

Although the ICESat satellite altimetry has uncertainty errors and the time delays related to the propagation of the pulse through the atmosphere and the ionosphere over 7 years, we have reconstructed the time series of water level or volume change based on GLAS data and lake area change. Compared to the in situ measurements data, the simultaneous GLAS footprints profiles of the L2B and L2C campaign are within the 99 % confidence interval and shown in Fig. 3. Over the period 2003–2009, we also compute the fluctuations in the GLAS-lake mean water level time series considering the water level seasonal trend removed during the same time span (see Fig. 4).

Glacier mass balance estimation

The change in heights of the lake water level is determined by the difference between the ICESat satellite orbit and the GLAS altimeter range distance measurement (Wang et al. 2013), with the addition of various corrections that take into account slope and roughness (Phan et al. 2014), correction for the geoid abnormal height effects on the Earth (Wu et al. 2014a). We can apply the Gaussian-Centroid (G-C) correction to fit the sample-weighted mean G-C offsets for each campaign (Lisano and Schutz 2001), suggesting that it is necessary to repeat earlier ICESat studies to estimate mass balance and evaluate if significant biases vary in different regions during the same campaigns (Borsa et al. 2014). The horizontal error (2.4 ± 7.3 m) and vertical error (0.04 ± 0.13 m) for the ICESat-GLAS data used are validated using similar glacier surface elevation (Carabajal and Harding 2005), compared to those for SRTM DEM v4.1 data.

Similar to the regional glacier mass balance, the overall bias (including returned waveform saturation, the established slope regression equation of slope, roughness with centroid elevation each GLAS footprint, co-registration bias (Nuth and Kääb 2011) as well as the inter-campaign

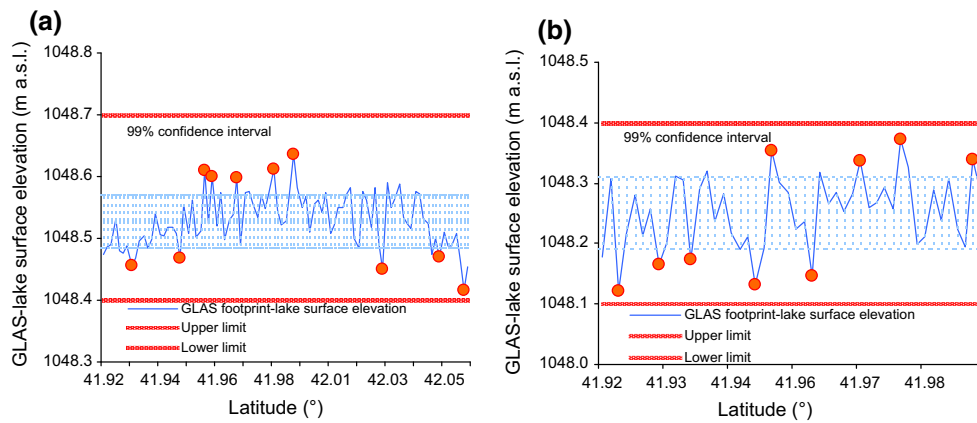


Fig. 3 **a** The GLAS footprints-lake water elevation profile variations in February 27, 2004 in the L2B campaign. **b** The GLAS footprints-lake water elevation profile variations in May 28, 2004 in the L2C campaign

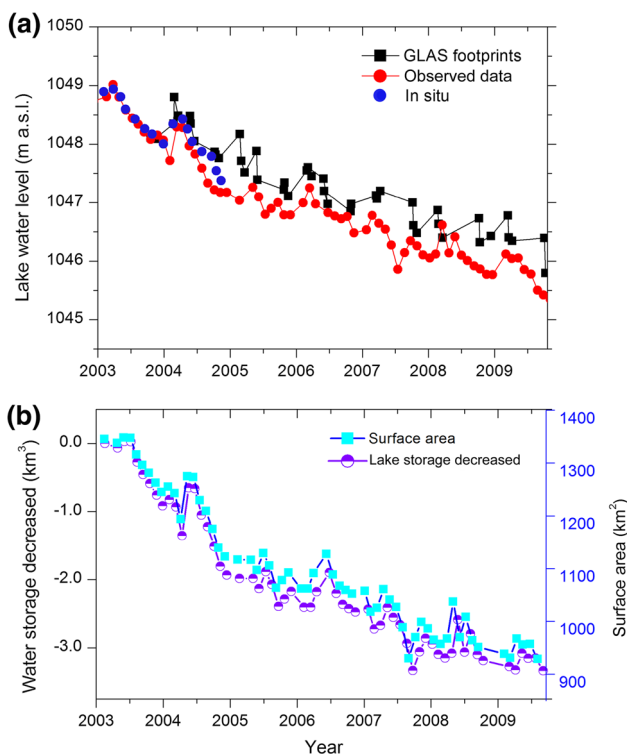


Fig. 4 **a** The comparison of Bosten lake water level change estimated by GLAS and observed measurements, where the observed time series data from Laboratoire d’Etudes en Géophysique et Océanographie Spatiales (LEGOS) and in situ measured water level data in this paper (Gao and Yao 2005); **b** the lake surface area and volume variations of the Bosten Lake over the period of 2003–2009

bias) is firstly calculated using the elevation differences of ICESat time series from 18 campaigns extracted on the basis of STRM DEM elevation. Secondly, the glacier surface cover classification and density parameter (Sørensen et al. 2011) were also computed based on GLAS waveforms, when the instantaneous firn, snow and glacier ice surface area from Landsat TM/ETM images containing

no cloud cover. Finally, the glacial mass balance in each 500 m altitudinal zone is calculated as (Wu et al. 2014b),

$$b_m = \frac{1}{S_m} (s_{\text{snow}} \times \rho_{\text{snow}} \times \Delta \bar{h}_{\text{snow}} + s_{\text{firn}} \times \rho_{\text{firn}} \times \Delta \bar{h}_{\text{firn}} + s_{\text{ice}} \times \rho_{\text{ice}} \times \Delta \bar{h}_{\text{ice}}), \tag{3}$$

where m is the t th altitudinal zone with an intervals of 500 m. S_m are glacier areas at intervals of 500 m in altitude. Snow density ρ_{snow} , firn density ρ_{firn} , and glacier ice density ρ_{ice} are assigned values of 350, 550, and 900 kg/m³, respectively (Ligtenberg et al. 2011). The variables $\Delta \bar{h}_{\text{snow}}$, $\Delta \bar{h}_{\text{firn}}$, $\Delta \bar{h}_{\text{ice}}$ indicate changes in elevations of snow, firn and glacier ice in each altitudinal zone, respectively, as estimated by GLAS waveform data. With respect to the ablation and short-term accumulation zone changes in the density profile, glacier mass balance is dominated by ice ablation where the mass change is in the non-steady-state (Ewert et al. 2012). The regional glacier mass balance b_g can be calculated by

$$b_g = \frac{1}{S} \sum_{t=1}^m S_m \times b_m = \frac{1}{S} \sum_{t=1}^m \sum_{i=1}^n s_i \times \rho_i \times \bar{h}_{i,m}, \tag{4}$$

where S is the entire mountain glacier areas. s_i is the different glacier-covered area in the altitudinal zone and the area-weighted average density ρ_i value includes glacier ice density ρ_{ice} , snow density ρ_{snow} , and firn density ρ_{firn} . t is the index of the altitudinal zone, $t = 1, 2, 3, \dots, m$. i is the number of each type of glacier surface covered, $i = 1, 2, 3, \dots, n$.

Uncertainty and errors

Validation of GLAS footprints-estimated lake level datasets suggests a statistical methodology for estimating the

instantaneous water level of GLAS footprint data compared to water level historical record in situ measurements. In this study, GLAS altimetry measurements and gauge level recorded for Bosten Lake water level were compared. The time series of gauge level data and the ERS-2 and ENVISAT satellite altimetry data are illustrated in Fig. 4. The Root-Mean-Square-Error (RMSE) and standard deviation of Bosten Lake were calculated using ENVISAT and ERS-2 measurements (Frappart et al. 2006a). In order to measuring the quality of geospatial data, the statistic variable $RMSE_e$ is used to evaluate the GLAS footprint elevation change along the ICESat orbital track:

$$RMSE_e = \sqrt{\frac{1}{n} \sum_{i=1}^n (z_{\text{footprints},i} - z_{\text{situ},i})^2}, \quad (5)$$

where $z_{\text{footprints},i}$ is the elevation of the i th estimated GLAS footprints in the any GLAS campaign dataset (m), $z_{\text{situ},i}$ is the elevation of the i th check point in the independent source with higher accuracy (m), n is the number of footprints being compared and $i = 1, 2, 3, \dots, n$. The relative bias (E_{bias}) is estimated as follows (Liu et al. 2011):

$$E_{\text{bias}} = \frac{1}{m} \sum_{j=1}^m \frac{x_{j,\text{footprints}} - x_{j,\text{situ}}}{x_{j,\text{footprints}}} \times 100 \%, \quad (6)$$

where m is the total number of GLAS footprints elevation profile, $x_{j,\text{footprints}}$ the GLAS-estimated elevation of lake water level and $x_{j,\text{situ}}$ the observed value of lake water level.

The uncertain error of lake water storage change calculated by GLAS data can be estimated by the following equation (Frappart et al. 2006b),

$$\delta V = \sum_{j=1}^m \delta s_j \times \delta h_j, \quad (7)$$

where δV is the error of the water storage change (ΔV), δs_j is the error of lake surface area change in the j th time span, and δh_j is the uncertainty error of lake water level change in the j th inter-campaign span, including the floating ice and waves on the lake water surface elevation profiles (the red circles shown in Fig. 3). The blue error bars show the water level fluctuations within the 99 % confidence interval and the red line is the GLAS data in vertical uncertainty.

Results and discussions

GLAS water level/elevation uncertainties

Comparing of in situ measurements (in blue circles) and GLAS-derived water level time series for Bosten Lake (Fig. 4a), demonstrates the two sets of lake water level variations (in situ measurements in blue, GLAS in black) are consistent, where their Pearson' correlation coefficient

is 0.96. The Bosten water level variation curve derived by GLAS data decreased by 2.31 ± 0.15 m while its in situ measurements data showed the water level decreased by 2.68 ± 0.20 m over the period of 2003–2009, which implies that the corresponding lake water storage decreased by 3.33 ± 0.25 km³. The difference between the water level derived from the GLAS data and in situ measurement data was 0.37 m, where the systematic errors are within the 99 % confidence level. Moreover, the two time series L2B and L2C from near the middle of Bosten Lake have a mean periodic amplitude in the range of approximately ± 0.15 m from peak to peak (Fig. 3a, b). The L2B elevation profile on February 27, 2004 is affected by floating ice, so the pulse peak bias is larger than the L2C campaign profile on May 28, 2004. In summary, GLAS footprint elevations from the ascending/descending track are significantly influenced by seasonal or extreme snowfall as well as melting ice during the freeze/thaw period when the uncertainty error of lake water surface fluctuations ($\delta h_{i,\text{footprint}}$) are within ± 0.15 m, in addition to the systematic error and co-registration bias of GLAS footprint data.

Lake water level and water storage changes

Figure 5 displays the water level variations of the Bosten and Ayding Lakes. The figure clearly shows that the water

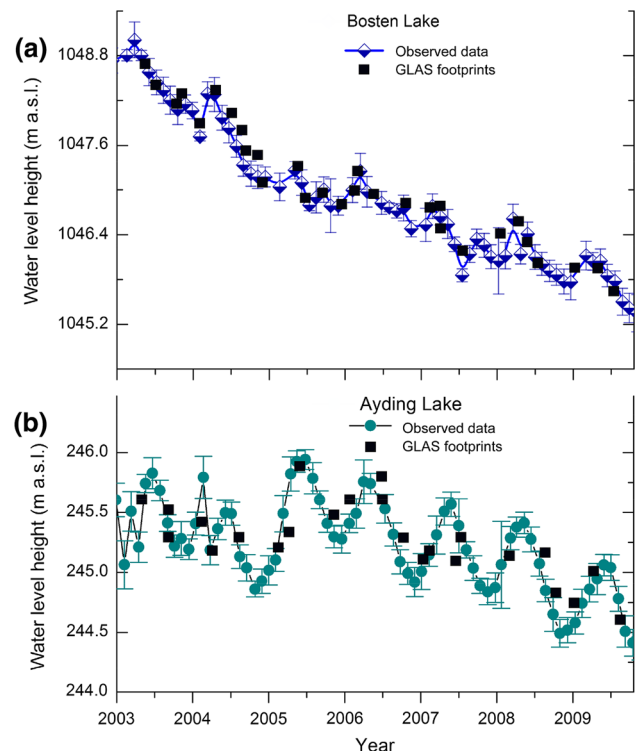


Fig. 5 The water level changes of the Bosten Lake (a) and Ayding Lake (b) estimated by GLAS and observed data over the period of 2003–2009

level of the Bosten Lake in October 2009 decreased by 2.68 ± 0.10 m compared to February 2003. However, the water level of the Ayding Lake increased in the period of 2003–2006, and decreased after 2006. The RMSE

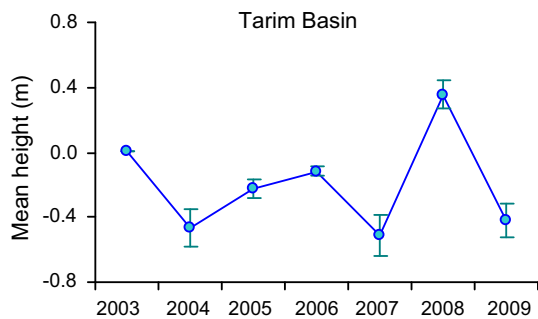


Fig. 6 The area-weighted average relative height variations of lakes in the Tarim Basin, China, over the period of 2003–2009

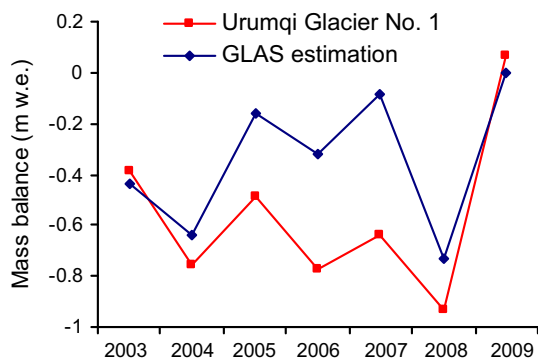


Fig. 7 The variations of the observed and GLAS-derived surface mass balance of the Glacier No. 1 at the source area of the Urumqi River during 2003–2009

difference between in situ observations and GLAS altimetry-derived lake mean water levels are 0.10 m and 0.12 m for the Bosten and Ayding Lake over the period of 2003–2009.

In view of Fig. 5, it is interesting that Ayding Lake water levels have greater seasonal fluctuations than in Bosten Lake. The lake water surface area of Aiding Lake decreased by approximately 50 km^2 compared to 2003, and correspondingly the GLAS-estimated lake water level decreased by 1.04 ± 0.3 m over the same time span. As a whole, the area-averaged water level height in the Tarim Basin also decreased by 0.41 ± 0.2 m (in Fig. 6) and correspondingly the lake water storage decreased by $13.85 \pm 6.2 \text{ km}^3$ w.e. compared to 2003. If the lakes water level and water storage continue to decline, some small lake may disappear, especially if the interactions between water withdrawal of human activity and lake recharge from precipitation and glacial meltwater are not balanced.

Glacier mass balance changes

Only one glacier in the East Tianshan Mountains is routinely observed, i.e., the Urumqi Glacier No. 1 at the upstream area of the Urumqi River. Although the glacier is not within the Tarim Basin, it is located near the boundary of the basin and in the upper catchment of the Bosten Lake. Therefore, its mass balance observation results may verify the glacier mass balance derived by the GLAS data. Figure 7 shows the GLAS-derived mass balance variations of the glaciers within 100 km from the Urumqi Glacier No.1 and the observed mass balance variations of the Urumqi Glacier No.1. Both variations are similar and highly

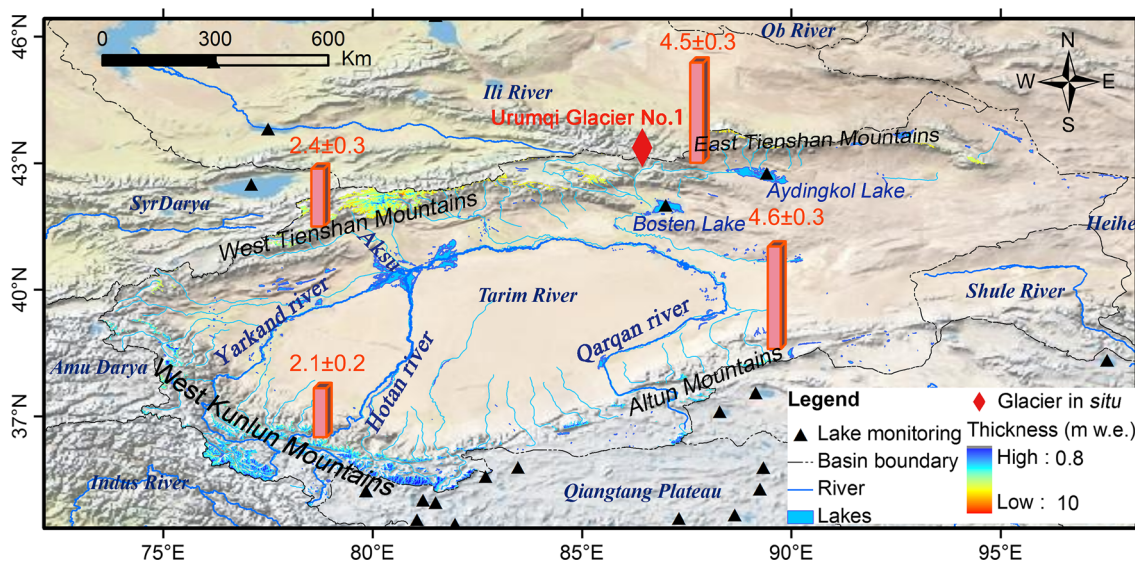


Fig. 8 The area-weighted height of the glacier surface elevation decreased in the mountains around the Tarim Basin over the period of 2003–2009

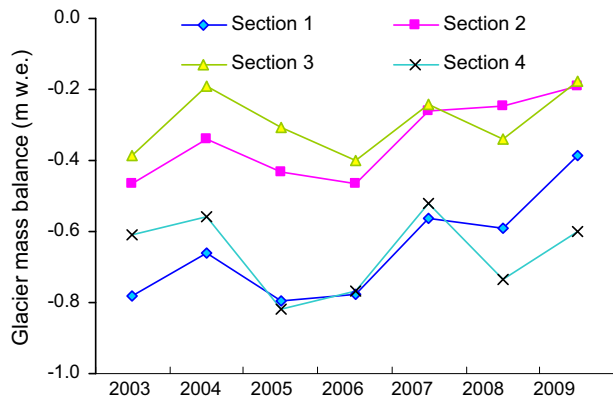


Fig. 9 The variations of the GLAS-derived mass balance of the glaciers in Sections 1, 2, 3, 4 over the period of 2003–2009

positively related (their multiple correlation coefficient is 0.75). This similarity indicates that the GLAS-derived mass balance is reliable.

Figures 8 and 9 present the GLAS-derived mass balance of the glaciers in 4 regions of the Tarim Basin over the period of 2003–2009. The cumulative glacier mass balance in the eastern Tarim Basin including Tianshan and Altun mountains is larger while smaller in the Kunlun Mountains in the western Tarim Basin. In the entire basin, the area-weighted average glacier thinning thickness was at a rate of 0.34 ± 0.25 m w.e./year, which is equivalent to 6.8 ± 1.2 km³ w.e. over the period 2003–2009.

Precipitation and evaporation

For hydrological storage changes (Döll et al. 2003), most of the world's catchment basins are in the WaterGap Global Hydrological Model (WGHM). As is known to all, the terrestrial water storage change of inland river basin depends on the net effect of precipitation (P) and evaporation (E), so P–E value has not only dominated the water mass change but also influenced on the land surface runoff change (Llovel et al. 2011). The inter-annual precipitation, evaporation, and P–E value variation of the entire basin, are shown in Fig. 10.

As Tarim river basin is located in an arid region, some of the small rivers are independent catchment and river stream disappeared into the desert. Thus, we have to use average annual runoff, evaporation and precipitation in this study. The annual surface runoff time series over 2003–2009 are well correlated to P–E curve, with Pearson's correlation coefficient of 0.81 at the significance level $\alpha < 0.01$, compared Figs. 10d and 11. It was observed that the P–E in Tarim River showed an increasing tendency, but there was a subtle decrease in evaporation fluctuations on the mountain regions. However, the total water mass

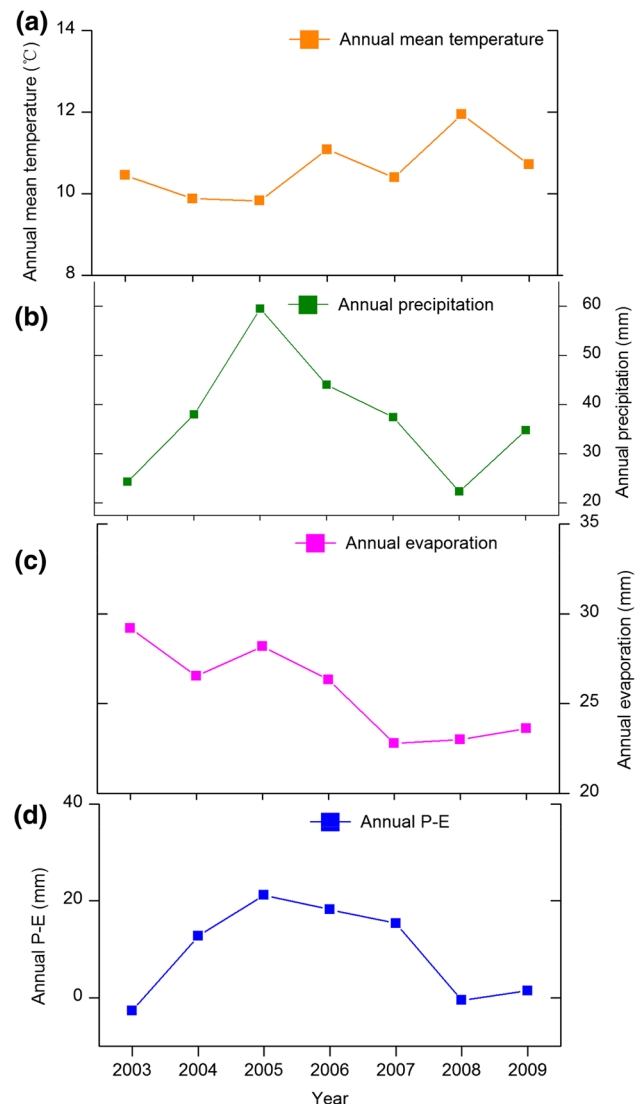


Fig. 10 Trend curves of annual mean temperature (a), annual precipitation (b), annual evaporation (c), and annual P–E value (d) in the entire Tarim Basin, 2003–2009. The NCEP/NCAR Reanalysis datasets of annual precipitation and evaporation are from National Oceanic and Atmospheric Administration Earth System Research Laboratory Physical Sciences Division (NOAA/ESRL PSD, see the website <http://www.esrl.noaa.gov/psd/data/reanalysis/index.html>), and these netCDF4-classic format data files are available for climatic anomalies analysis in the basin

storage from P–E value was actually increasing during 2003–2009, and increased by at least 10 mm water equivalent in entire basin. Hence, the spatial difference in entire basin might be due to the effect by regional climatic anomalies (in Fig. 12).

According to Figs. 9 and 11, the fluctuations of GLAS-regional glacier mass balance and surface runoff were in the opposite. When the regional glacier mass loss is larger, the glacial runoff is larger, especially in 2005–2006. In view of Figs. 10b and 11, both of precipitation and P–E

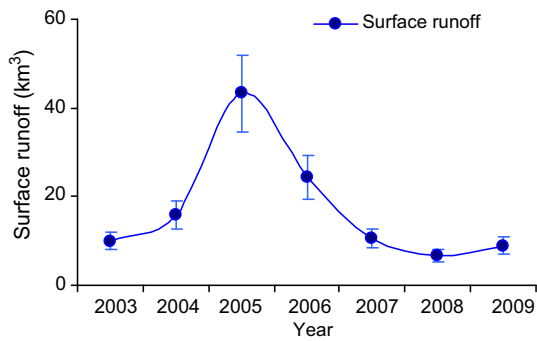


Fig. 11 The annual surface runoff variations in the entire Tarim Basin, 2003–2009, from WaterGAP (Water-Global Analysis and Prognosis) model developed at the Center for Environmental Systems Research, University of Kasse, and the other available components of the hydrological cycle at URL: <https://www.uni-frankfurt.de/45218063/WaterGAP>

change play an important role at the seasonal and annual scales (Kundzewicz et al. 2015), rather than temperature change. Due to the limited data of climatic change and GLAS-glacier mass balance, we could not further study the mechanism of climatic anomalies affecting the surface runoff (Hao et al. 2008) and an indistinctive trend of river discharge (Yaning et al. 2009).

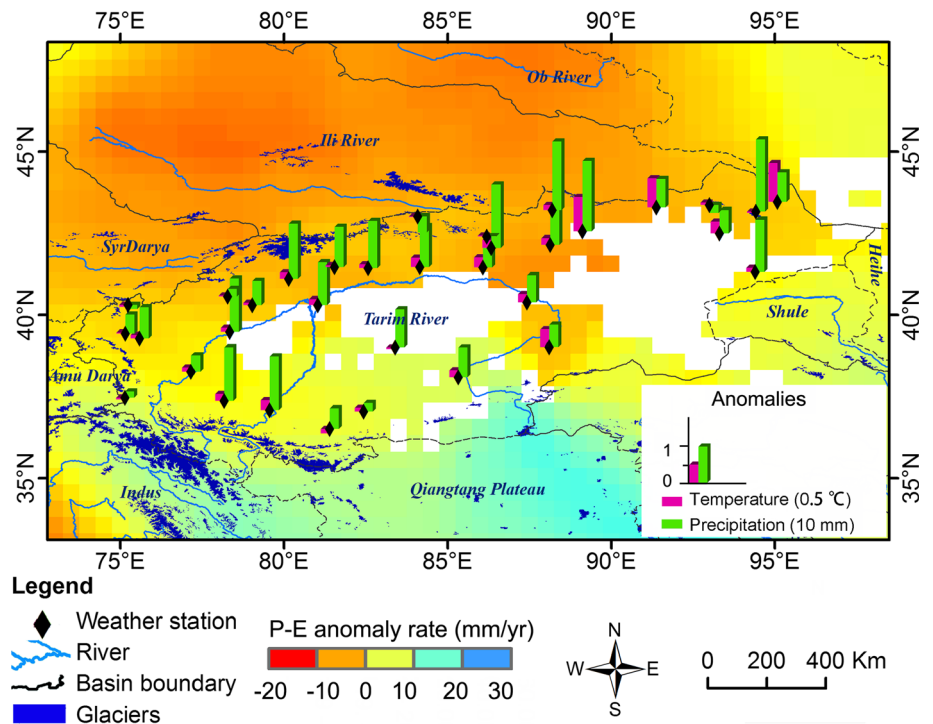
In view of Figs. 9 and 11, it was interesting to note that both of annual temperature and precipitation showed an obvious tendency of increase during 2003–2009. Comparisons of 33 weather station climatic anomalies seem that

the annual mean temperature increase dominated the glacier mass loss, and are consistent with regional GLAS-glacier mass balance (in Fig. 12). Furthermore, the East Tianshan Mountains glacier thinning height is largest in Tarim Basin on account of annual mean temperature increased by 0.8 °C compared to 2003; and the West Kunlun Mountains glacier mass thinning height is less. The reason is that the P–E in West Kunlun Mountains has shown a slightly positive trend and accordingly the regional glacier mass balance is less although the mean annual temperature is continually increasing variations.

Effect of glacier mass loss on glacial meltwater and lake water storage

In inland river basins, changes in glacier mass balance not only influence glacier meltwater, but can also affect the “close lake”. In the Tarim Basin, the glacier runoff accounts for at least 41.5 % of the total river runoff (Gao et al. 2010). This amount suggest that runoff changes in this basin should be significantly affected by glacier melt, especially in climatic anomalies (Werth and Güntner 2010). A recent study revealed that streamflows in the Aksu River and the Yarkant River have significantly ($P < 0.05$) increased (Chen et al. 2006). This increased trend might be the result of the recent glacier mass loss. It was estimated that total glacial meltwater runoff increased by 14.3 % in the inland river basins in northwest China with a temperature rise of 0.03 °C/year (Ersi et al. 2010).

Fig. 12 The spatial distribution map of annual P–E anomaly rate change in Tarim Basin, 2003–2009. The 33 weather stations datasets of increased temperature and precipitation observed are downloaded from China Meteorological Data Sharing Service System (URL: <http://www.cdc.nmic.cn/home.do>), which the temperature and precipitation anomalies deviated from some average referred to as climatic anomaly (Jones and Hulme 1996)



Usually, glacier mass loss accurate acceralte and increased river runoff can lead to an increase in water storage in the “close lakes.” However, our study showed that the water storage of lakes in the Tarim Basin generally decreased. This difference is largely caused by the consumption of water resources by the human activities (Gao and Yao 2005) (land use, oases area expansion, population growth, river damming, industrial water consumption and agricultural irrigation, etc.), except ecological condition (Zhao et al. 2013a) and global climate change (Karthé et al. 2015).

Conclusions

The study of water resources has drawn much attention, especially in arid regions. Multiple global space-borne satellites provide a useful method for this study. In the Tarim Basin, the shortage of water resources is a serious handicap social, economic, and environmental development. Glaciers in the high mountains around the basin function as “solid reservoirs.” However, their mass balance change and effect on the water resources are not clear. In this paper, we used the GLAS data and high-resolution satellite images to estimate the changes of glaciers and lakes in the Tarim Basin. Comparing the GLAS-derived mass balance and lake water levels with observational data, we determined the derived datasets are reliable. Through comprehensive computations and analyses, we revealed that the rate of the glacier mass loss differs spatially where the Tianshan and Altun Mountains to the east of the Tarim Basin are melting faster than the Kunlun Mountains to the west of the basin. The area-weighted average glacier thinning occurred at a rate of 0.34 ± 0.25 m w.e./year over the period 2003–2009. However, the mean water level of lakes decreased by 0.41 ± 0.25 m compared to 2003. This water level decrease implies water consumption by human activities and agricultural irrigation in the oases of the basin. Therefore, it is urgent to study of the effects of glacial meltwater runoff changes under global warming on water resources in order to sustainably develop water resources in arid central Asia.

Acknowledgments This study was completed with the support of the National Natural Science Foundation Project of China (Grant No. 41190084) and the Strategic Science and Technology Program of Chinese Academy of Sciences (grant No. XDB03030204). We thank Laboratoire d'Etudes en Géophysique et Océanographie Spatiales (LEGOS, HYDROWEB: <http://www.legos.obs-mip.fr/en>) in Toulouse for providing the Bosten, Top lakes monitoring data, as well as the U.S. Geological Survey providing hydrographic mapping product with HydroSHEDS data (<http://www.hydrosheds.cr.usgs.gov/index.php>) and Landsat TM/ETM imageries (<http://www.earthexplorer.usgs.gov/>). Furthermore, the authors should like to thank four anonymous reviewers and editors for these massive suggestions and

various efforts. We also thank Prof. F.G. Lemoine from Planetary Geodynamics Laboratory, NASA GSFC for giving the technological supports on the times series of lake water level weekly using GLAS altimeter data from 2003 to 2009 for ITRF2008 information. We thank J.F. Crétaux for having available ERS-2/ENVISAT altimetry data of lakes on the studies.

References

- Abdallah H, Bailly J-S, Baghdadi N, Lemarquand N (2011) Improving the assessment of ICESat water altimetry accuracy accounting for autocorrelation. *ISPRS J Photogramm Remote Sens* 66(6):833–844. doi:10.1016/j.isprsjprs.2011.09.002
- Abshire JB, Sun X, Riris H, Sirota JM, McGarry JF, Palm S, Yi D, Liiva P (2005) Geoscience Laser Altimeter System (GLAS) on the ICESat Mission: On-orbit measurement performance. *Geophys Res Lett* 32(21):L21S02. doi:10.1029/2005GL024028
- Alsodf DE, Rodríguez E, Lettenmaier DP (2007) Measuring surface water from space. *Rev Geophys* 45(2):RG2002. doi:10.1029/2006RG000197
- Baghdadi N, Lemarquand N, Abdallah H, Bailly JS (2011) The relevance of GLAS/ICESat elevation data for the monitoring of river networks. *Remote Sens* 3(4):708–720. doi:10.3390/rs3040708
- Beniston M (2003) Climatic change in mountain regions: a review of possible impacts. In: Diaz H (ed) *Climate variability and change in high elevation regions: past, present & future*. Advances in global change research, vol 15. Springer, Netherlands, pp 5–31
- Biemans H, Haddeland I, Kabat P, Ludwig F, Hutjes RWA, Heinke J, von Bloh W, Gerten D (2011) Impact of reservoirs on river discharge and irrigation water supply during the 20th century. *Water Resour Res* 47(3):W03509. doi:10.1029/2009WR008929
- Borsa AA, Moholdt G, Fricker HA, Brunt KM (2014) A range correction for ICESat and its potential impact on ice-sheet mass balance studies. *Cryosphere* 8(2):345–357. doi:10.5194/tc-8-345-2014
- Calmant S, Seyler F (2006) Continental surface waters from satellite altimetry. *CR Geosci* 338(14–15):1113–1122. doi:10.1016/j.crte.2006.05.012
- Calmant S, Seyler F, Crétaux J (2008) Monitoring continental surface waters by satellite altimetry. *Surv Geophys* 29(4–5):247–269. doi:10.1007/s10712-008-9051-1
- Carabajal CC, Harding DJ (2005) ICESat validation of SRTM C-band digital elevation models. *Geophys Res Lett* 32(22):2. doi:10.1029/2005GL023957
- Chen Y, Takeuchi K, Xu C, Chen Y, Xu Z (2006) Regional climate change and its effects on river runoff in the Tarim Basin, China. *Hydrol Process* 20(10):2207–2216. doi:10.1002/hyp.6200
- Crétaux J-F, Birkett C (2006) Lake studies from satellite radar altimetry. *CR Geosci* 338(14–15):1098–1112. doi:10.1016/j.crte.2006.08.002
- Crétaux JF, Jelinski W, Calmant S, Kouraev A, Vuglinski V, Bergé-Nguyen M, Gennero MC, Nino F, Abarca Del Rio R, Cazenave A, Maisongrande P (2011) SOLS: a lake database to monitor in the Near Real Time water level and storage variations from remote sensing data. *Adv Space Res* 47(9):1497–1507. doi:10.1016/j.asr.2011.01.004
- Da Silva JS, Seyler F, Calmant S, Rotunno Filho OC, Roux E, Araújo AAM, Guyot JL (2011) Water level dynamics of Amazon wetlands at the watershed scale by satellite altimetry. *Int J Remote Sens* 33(11):3323–3353. doi:10.1080/01431161.2010.531914
- Döll P, Kaspar F, Lehner B (2003) A global hydrological model for deriving water availability indicators: model tuning and

- validation. *J Hydrol* 270(1–2):105–134. doi:[10.1016/S0022-1694\(02\)00283-4](https://doi.org/10.1016/S0022-1694(02)00283-4)
- Ersi K, Chaohai L, Zichu X, Xin L, Yongping S (2010) Assessment of glacier water resources based on the glacier inventory of China. *Ann Glaciol* 50(53):104–110. doi:[10.3189/172756410790595822](https://doi.org/10.3189/172756410790595822)
- Ewert H, Groh A, Dietrich R (2012) Volume and mass changes of the Greenland ice sheet inferred from ICESat and GRACE. *J Geodyn* 59–60:111–123. doi:[10.1016/j.jog.2011.06.003](https://doi.org/10.1016/j.jog.2011.06.003)
- Frappart F, Calmant S, Cauhopé M, Seyler F, Cazenave A (2006a) Preliminary results of ENVISAT RA-2-derived water levels validation over the Amazon basin. *Remote Sens Environ* 100(2):252–264. doi:[10.1016/j.rse.2005.10.027](https://doi.org/10.1016/j.rse.2005.10.027)
- Frappart F, Minh KD, L’Hermite J, Cazenave A, Ramillien G, Le Toan T, Mognard-Campbell N (2006b) Water volume change in the lower Mekong from satellite altimetry and imagery data. *Geophys J Int* 167(2):570–584. doi:[10.1111/j.1365-246X.2006.03184.x](https://doi.org/10.1111/j.1365-246X.2006.03184.x)
- Gao H, Yao Y (2005) Quantitative effect of human activities on water level change of bosten lake in recent 50 years. *Sci Geogr Sinica* 25(3):305–309 (in Chinese)
- Gao X, Ye B, Zhang S, Qiao C, Zhang X (2010) Glacier runoff variation and its influence on river runoff during 1961–2006 in the Tarim River Basin, China. *Sci Chin Earth Sci* 53(6):880–891. doi:[10.1007/s11430-010-0073-4](https://doi.org/10.1007/s11430-010-0073-4)
- Hao X, Chen Y, Xu C, Li W (2008) Impacts of climate change and human activities on the surface runoff in the Tarim River Basin over the last fifty years. *Water Resour Manage* 22(9):1159–1171. doi:[10.1007/s11269-007-9218-4](https://doi.org/10.1007/s11269-007-9218-4)
- Hirt C, Marti U, Bürki B, Featherstone WE (2010) Assessment of EGM2008 in Europe using accurate astrogeodetic vertical deflections and omission error estimates from SRTM/DTM2006.0 residual terrain model data. *J Geophys Res Solid Earth* 115(B10):B10404. doi:[10.1029/2009JB007057](https://doi.org/10.1029/2009JB007057)
- Immerzeel WW, van Beek LPH, Bierkens MFP (2010) Climate change will affect the Asian water towers. *Science* 328(5984):1382–1385. doi:[10.1126/science.1183188](https://doi.org/10.1126/science.1183188)
- Jing Z, Jiao K, Yao T, Wang N, Li Z (2006) Mass balance and recession of Úrümqi glacier No. 1, Tien Shan, China, over the last 45 years. *Ann Glaciol* 43(1):214–217. doi:[10.3189/172756406781811899](https://doi.org/10.3189/172756406781811899)
- Jones PD, Hulme M (1996) Calculating regional climatic time series for temperature and precipitation: methods and illustrations. *Int J Climatol* 16(4):361–377. doi:[10.1002/\(SICI\)1097-0088\(199604\)16:4<361:AID-JOC53>3.0.CO;2-F](https://doi.org/10.1002/(SICI)1097-0088(199604)16:4<361:AID-JOC53>3.0.CO;2-F)
- Karthe D, Chalov S, Borchardt D (2015) Water resources and their management in central Asia in the early twenty first century: status, challenges and future prospects. *Environ Earth Sci* 73(2):487–499. doi:[10.1007/s12665-014-3789-1](https://doi.org/10.1007/s12665-014-3789-1)
- Kropáček J, Braun A, Kang S, Feng C, Ye Q, Hochschild V (2012) Analysis of lake level changes in Nam Co in central Tibet utilizing synergistic satellite altimetry and optical imagery. *Int J Appl Earth Obs Geoinf* 17:3–11. doi:[10.1016/j.jag.2011.10.001](https://doi.org/10.1016/j.jag.2011.10.001)
- Kundzewicz ZW, Merz B, Vorogushyn S, Hartmann H, Duethmann D, Wortmann M, Huang S, Su B, Jiang T, Krysanova V (2015) Analysis of changes in climate and river discharge with focus on seasonal runoff predictability in the Aksu River Basin. *Environ Earth Sci* 73(2):501–516. doi:[10.1007/s12665-014-3137-5](https://doi.org/10.1007/s12665-014-3137-5)
- Landerer FW, Swenson SC (2012) Accuracy of scaled GRACE terrestrial water storage estimates. *Water Resour Res* 48(4):W04531. doi:[10.1029/2011WR011453](https://doi.org/10.1029/2011WR011453)
- Lemoine FG, Zelensky NP, Chinn DS, Pavlis DE, Rowlands DD, Beckley BD, Luthcke SB, Willis P, Ziebart M, Sibthorpe A, Boy JP, Luceri V (2010) Towards development of a consistent orbit series for TOPEX, Jason-1, and Jason-2. *Adv Space Res* 46(12):1513–1540. doi:[10.1016/j.asr.2010.05.007](https://doi.org/10.1016/j.asr.2010.05.007)
- Li X, Williams MW (2008) Snowmelt runoff modelling in an arid mountain watershed, Tarim Basin, China. *Hydrol Process* 22(19):3931–3940. doi:[10.1002/hyp.7098](https://doi.org/10.1002/hyp.7098)
- Li X, Xu L, Tian X, Kong D (2012) Terrain slope estimation within footprint from ICESat/GLAS waveform: model and method. *J Appl Remote Sens* 6(1):063534–063534. doi:[10.1117/1.JRS.6.063534](https://doi.org/10.1117/1.JRS.6.063534)
- Ligtenberg SRM, Helsen MM, van den Broeke MR (2011) An improved semi-empirical model for the densification of Antarctic firn. *Cryosphere* 5(4):809–819. doi:[10.5194/tc-5-809-2011](https://doi.org/10.5194/tc-5-809-2011)
- Lisano ME, Schutz BE (2001) Arcsecond-level pointing calibration for ICESat laser altimetry of ice sheets. *J Geodesy* 75(2–3):99–108. doi:[10.1007/s001900000156](https://doi.org/10.1007/s001900000156)
- Liu S, Ding Y, Shangguan D, Zhang Y, Li J, Han H, Wang J, Xie C (2006) Glacier retreat as a result of climate warming and increased precipitation in the Tarim river basin, northwest China. *Ann Glaciol* 43(1):91–96. doi:[10.3189/172756406781812168](https://doi.org/10.3189/172756406781812168)
- Liu T, Willems P, Pan XL, Bao AM, Chen X, Veroustraete F, Dong QH (2011) Climate change impact on water resource extremes in a headwater region of the Tarim basin in China. *Hydrol Earth Syst Sci* 15(11):3511–3527. doi:[10.5194/hess-15-3511-2011](https://doi.org/10.5194/hess-15-3511-2011)
- Llovel W, Becker M, Cazenave A, Crétaux J-F, Ramillien G (2010) Global land water storage change from GRACE over 2002–2009; Inference on sea level. *CR Geosci* 342(3):179–188. doi:[10.1016/j.crte.2009.12.004](https://doi.org/10.1016/j.crte.2009.12.004)
- Llovel W, Becker M, Cazenave A, Jevrejeva S, Alkama R, Decharme B, Douville H, Ablain M, Beckley B (2011) Terrestrial waters and sea level variations on interannual time scale. *Global Planet Change* 75(1–2):76–82. doi:[10.1016/j.gloplacha.2010.10.008](https://doi.org/10.1016/j.gloplacha.2010.10.008)
- Los SO, Rosette JAB, Kljun N, North PRJ, Chasmer L, Suárez JC, Hopkinson C, Hill RA, van Gorsel E, Mahoney C, Berni JAJ (2012) Vegetation height and cover fraction between 60°S and 60°N from ICESat GLAS data. *Geosci Model Develop* 5(2):413–432. doi:[10.5194/gmd-5-413-2012](https://doi.org/10.5194/gmd-5-413-2012)
- McFeeters SK (1996) The use of the normalized difference water index (NDWI) in the delineation of open water features. *Int J Remote Sens* 17(7):1425–1432. doi:[10.1080/01431169608948714](https://doi.org/10.1080/01431169608948714)
- Medina CE, Gomez-Enri J, Alonso JJ, Villares P (2008) Water level fluctuations derived from ENVISAT Radar Altimeter (RA-2) and in situ measurements in a subtropical waterbody: Lake Izabal (Guatemala). *Remote Sens Environ* 112(9):3604–3617. doi:[10.1016/j.rse.2008.05.001](https://doi.org/10.1016/j.rse.2008.05.001)
- Moiwo JP, Yang Y, Tao F, Lu W, Han S (2011) Water storage change in the Himalayas from the Gravity Recovery and Climate Experiment (GRACE) and an empirical climate model. *Water Resour Res* 47(7):W07521. doi:[10.1029/2010WR010157](https://doi.org/10.1029/2010WR010157)
- Nuth C, Kääb A (2011) Co-registration and bias corrections of satellite elevation data sets for quantifying glacier thickness change. *Cryosphere* 5(1):271–290. doi:[10.5194/tc-5-271-2011](https://doi.org/10.5194/tc-5-271-2011)
- Pavlis NK, Holmes SA, Kenyon SC, Factor JK (2012) The development and evaluation of the Earth Gravitational Model 2008 (EGM2008). *J Geophys Res Solid Earth* 117(B4):B04406. doi:[10.1029/2011JB008916](https://doi.org/10.1029/2011JB008916)
- Phan VH, Lindenbergh R, Menenti M (2012) ICESat derived elevation changes of Tibetan lakes between 2003 and 2009. *Int J Appl Earth Obs Geoinf* 17:12–22. doi:[10.1016/j.jag.2011.09.015](https://doi.org/10.1016/j.jag.2011.09.015)
- Phan VH, Lindenbergh RC, Menenti M (2014) Orientation dependent glacial changes at the Tibetan Plateau derived from 2003–2009 ICESat laser altimetry. *Cryosphere Discuss* 8(3):2425–2463. doi:[10.5194/tcd-8-2425-2014](https://doi.org/10.5194/tcd-8-2425-2014)
- Piao S, Ciais P, Huang Y, Shen Z, Peng S, Li J, Zhou L, Liu H, Ma Y, Ding Y, Friedlingstein P, Liu C, Tan K, Yu Y, Zhang T, Fang J (2010) The impacts of climate change on water resources and agriculture in China. *Nature* 467(7311):43–51. doi:[10.1038/nature09364](https://doi.org/10.1038/nature09364)

- Qi F, Wei L, Jianhua S, Yonghong S, Yewu Z, Zongqiang C, Haiyang X (2005) Environmental effects of water resource development and use in the Tarim River basin of northwestern China. *Environ Geol* 48(2):202–210. doi:[10.1007/s00254-005-1288-0](https://doi.org/10.1007/s00254-005-1288-0)
- Raup B, Kääb A, Kargel JS, Bishop MP, Hamilton G, Lee E, Paul F, Rau F, Soltesz D, Khalsa SJS, Beedle M, Helm C (2007a) Remote sensing and GIS technology in the Global Land Ice Measurements from Space (GLIMS) Project. *Comput Geosci* 33(1):104–125. doi:[10.1016/j.cageo.2006.05.015](https://doi.org/10.1016/j.cageo.2006.05.015)
- Raup B, Racoviteanu A, Khalsa SJS, Helm C, Armstrong R, Arnaud Y (2007b) The GLIMS geospatial glacier database: A new tool for studying glacier change. *Glob Planet Change* 56(1–2):101–110. doi:[10.1016/j.gloplacha.2006.07.018](https://doi.org/10.1016/j.gloplacha.2006.07.018)
- Santos da Silva J, Calmant S, Seyler F, Rotunno Filho OC, Cochonneau G, Mansur WJ (2010) Water levels in the Amazon basin derived from the ERS 2 and ENVISAT radar altimetry missions. *Remote Sens Environ* 114(10):2160–2181. doi:[10.1016/j.rse.2010.04.020](https://doi.org/10.1016/j.rse.2010.04.020)
- Schutz BE, Zwally HJ, Shuman CA, Hancock D, DiMarzio JP (2005) Overview of the ICESat Mission. *Geophys Res Lett* 32(21):L21S01. doi:[10.1029/2005GL024009](https://doi.org/10.1029/2005GL024009)
- Song C, Huang B, Richards K, Ke L, Hien Phan V (2014) Accelerated lake expansion on the Tibetan Plateau in the 2000s: induced by glacial melting or other processes? *Water Resour Res* 50(4):3170–3186. doi:[10.1002/2013WR014724](https://doi.org/10.1002/2013WR014724)
- Sørensen LS, Simonsen SB, Nielsen K, Lucas-Picher P, Spada G, Adalgeirsdóttir G, Forsberg R, Hvidberg CS (2011) Mass balance of the Greenland ice sheet (2003–2008) from ICESat data—the impact of interpolation, sampling and firn density. *Cryosphere* 5(1):173–186. doi:[10.5194/tc-5-173-2011](https://doi.org/10.5194/tc-5-173-2011)
- Sorg A, Bolch T, Stoffel M, Solomina O, Beniston M (2012) Climate change impacts on glaciers and runoff in Tien Shan (Central Asia). *Nature Climate Change* 2(10):725–731. doi:[10.1038/nclimate1592](https://doi.org/10.1038/nclimate1592)
- Verpoorter C, Kutser T, Seekell DA, Tranvik LJ (2014) A global inventory of lakes based on high-resolution satellite imagery. *Geophys Res Lett* 41(18):GL060641. doi:[10.1002/2014GL060641](https://doi.org/10.1002/2014GL060641)
- Wang X, Gong P, Zhao Y, Xu Y, Cheng X, Niu Z, Luo Z, Huang H, Sun F, Li X (2013) Water-level changes in China's large lakes determined from ICESat/GLAS data. *Remote Sens Environ* 132:131–144. doi:[10.1016/j.rse.2013.01.005](https://doi.org/10.1016/j.rse.2013.01.005)
- Werth S, Güntner A (2010) Calibration analysis for water storage variability of the global hydrological model WGHM. *Hydrol Earth Syst Sci* 14(1):59–78. doi:[10.5194/hess-14-59-2010](https://doi.org/10.5194/hess-14-59-2010)
- Wisser D, Froelking S, Hagen S, Bierkens MFP (2013) Beyond peak reservoir storage? A global estimate of declining water storage capacity in large reservoirs. *Water Resour Res* 49(9):5732–5739. doi:[10.1002/wrcr.20452](https://doi.org/10.1002/wrcr.20452)
- Wu H, Wang N, Guo Z, Wu Y (2014a) Regional glacier mass loss estimated by ICESat–GLAS data and SRTM digital elevation model in the West Kunlun Mountains, Tibetan Plateau, 2003–2009. *J Appl Remote Sens* 8(1):083515–083515. doi:[10.1117/1.JRS.8.083515](https://doi.org/10.1117/1.JRS.8.083515)
- Wu H, Wang N, Jiang X, Guo Z (2014b) Variations in water level and glacier mass balance in Nam Co lake, Nyainqentanglha range, Tibetan Plateau, based on ICESat data for 2003–09. *Ann Glaciol* 55(66):239–247. doi:[10.3189/2014AoG66A100](https://doi.org/10.3189/2014AoG66A100)
- Yanling C, Changchun X, Xingming H, Weihong L, Yapeng C, Chenggang Z, Zhaoxia Y (2009) Fifty-year climate change and its effect on annual runoff in the Tarim River Basin, China. *Quat Int* 208(1–2):53–61. doi:[10.1016/j.quaint.2008.11.011](https://doi.org/10.1016/j.quaint.2008.11.011)
- Ye B, Yang D, Jiao K, Han T, Jin Z, Yang H, Li Z (2005) The Urumqi River source Glacier No. 1, Tianshan, China: changes over the past 45 years. *Geophys Res Lett* 32(21):L21504. doi:[10.1029/2005GL024178](https://doi.org/10.1029/2005GL024178)
- Zelensky N, Berthias J-P, Lemoine F (2006) DORIS time bias estimated using Jason-1, TOPEX/Poseidon and ENVISAT orbits. *J Geodesy* 80(8–11):497–506. doi:[10.1007/s00190-006-0075-3](https://doi.org/10.1007/s00190-006-0075-3)
- Zelensky N, Lemoine F, Chinn D, Melachroinos S, Beckley B, Beall J, Bordyugov O (2014) Estimated SLR station position and network frame sensitivity to time-varying gravity. *J Geodesy* 88(6):517–537. doi:[10.1007/s00190-014-0701-4](https://doi.org/10.1007/s00190-014-0701-4)
- Zhang Q, Xu C-Y, Tao H, Jiang T, Chen Y (2010) Climate changes and their impacts on water resources in the arid regions: a case study of the Tarim River basin, China. *Stoch Environ Res Risk Assess* 24(3):349–358. doi:[10.1007/s00477-009-0324-0](https://doi.org/10.1007/s00477-009-0324-0)
- Zhang G, Xie H, Kang S, Yi D, Ackley SF (2011) Monitoring lake level changes on the Tibetan Plateau using ICESat altimetry data (2003–2009). *Remote Sens Environ* 115(7):1733–1742. doi:[10.1016/j.rse.2011.03.005](https://doi.org/10.1016/j.rse.2011.03.005)
- Zhang S, Gao H, Naz BS (2014) Monitoring reservoir storage in South Asia from multisatellite remote sensing. *Water Resour Res* 50(11):8927–8943. doi:[10.1002/2014WR015829](https://doi.org/10.1002/2014WR015829)
- Zhao R, Chen Y, Shi P, Zhang L, Pan J, Zhao H (2013a) Land use and land cover change and driving mechanism in the arid inland river basin: a case study of Tarim River, Xinjiang, China. *Environ Earth Sci* 68(2):591–604. doi:[10.1007/s12665-012-1763-3](https://doi.org/10.1007/s12665-012-1763-3)
- Zhao Y, Li H, Huang A, He Q, Huo W, Wang M (2013b) Relationship between thermal anomalies in Tibetan Plateau and summer dust storm frequency over Tarim Basin, China. *J Arid Land* 5(1):25–31. doi:[10.1007/s40333-013-0138-2](https://doi.org/10.1007/s40333-013-0138-2)
- Zwally HJ, Schutz B, Abdalati W, Abshire J, Bentley C, Brenner A, Bufton J, Dezio J, Hancock D, Harding D, Herring T, Minster B, Quinn K, Palm S, Spinhrne J, Thomas R (2002) ICESat's laser measurements of polar ice, atmosphere, ocean, and land. *J Geodyn* 34(3–4):405–445. doi:[10.1016/S0264-3707\(02\)00042-X](https://doi.org/10.1016/S0264-3707(02)00042-X)